Electroweak Measurements of Neutron Densities in PREX and CREX at JLab, USA

ROBERT MICHAELS[1]

Thomas Jefferson National Accelerator Laboratory
12000 Jefferson Ave, Newport News, VA 23606 USA

Measurement of the parity-violating electron scattering asymmetry from ^{208}Pb has demonstrated a new opportunity at Jefferson Lab to measure the weak charge distribution and hence pin down the neutron radius in nuclei in a relatively clean and model-independent way. This is because the Z boson of the weak interaction couples primarily to neutrons. We will describe the PREX and CREX experiments on ^{208}Pb and ^{48}Ca respectively. PREX-I ran in 2010, and CREX and a second run of PREX are currently in preparation.

PRESENTED AT

Twelfth Conference on the Intersections of Particle and
Nuclear Physics
Vail, Colorado, USA May 19–24, 2015

1 Parity-Violating Measurements of Neutron Densities

Historically, electromagnetic scattering has accurately measured the charge distribution of nuclei [1, 2], providing a detailed picture of the atomic nucleus. Proton radii have been determined accurately for many nuclei using electron scattering experiments [1, 2, 3]. This accuracy reflects the accuracy of perturbative treatments of the electromagnetic process. The neutron density distribution is more difficult to measure accurately because it interacts mainly with hadronic probes (pions [4], protons [5, 6, 7], antiprotons [8, 9], and alphas [10, 11]) through nonperturbative interactions, the theoretical description of which is model-dependent. Other approaches to inferring R_n include inelastic scattering excitation of giant dipole resonances [12, 13] and atomic mass fits [14, 15]. Neutron radii can also be measured with neutrino-nucleus elastic scattering [16, 17].

Parity violating electron scattering measures the asymmetry

$$A_{PV} = \frac{\sigma_R - \sigma_L}{\sigma_R + \sigma_L} \tag{1}$$

where $\sigma_{R(L)}$ is the cross section for right (left)-handed helicity of the incident electrons, is very small, of order one part per million (ppm).

This asymmetry provides a model independent probe of neutron densities that is free from most strong interaction uncertainties. The Z^0 boson, which carries the weak force, couples primarily to neutrons. In the Born approximation, A_{PV}, is

$$A_{PV} \approx \frac{G_F Q^2}{4\pi\alpha\sqrt{2}} \frac{F_W(Q^2)}{F_{ch}(Q^2)} \tag{2}$$

where G_F is the Fermi constant, α the fine structure constant, and $F_{ch}(Q^2)$ is the Fourier transform of the known charge density. The asymmetry is proportional to the weak form factor $F_W(Q^2)$. This is closely related to the Fourier transform of the neutron density, and therefore the neutron density can be extracted from an electro-weak measurement [18]

$$A_{pv} \approx \frac{G_F Q^2}{4\pi\alpha\sqrt{2}} \left[1 - 4\sin^2\theta_W - \frac{F_n(Q^2)}{F_{ch}(Q^2)} \right] \tag{3}$$

Corrections to the Born approximation from Coulomb distortion effects must be included and have been accurately calculated [19], and other theoretical interpretation issues have been considered in [20].

The weak form factor is the Fourier transform of the weak charge density $\rho_W(r)$,

$$F_W(Q^2) = \frac{1}{Q_W} \int d^3r \frac{\sin Qr}{Qr} \rho_W(r), \tag{4}$$

and is normalized $F(Q = 0) = 1$. The total weak charge of the nucleus is $Q_W = \int d^3 r \rho_W(r)$.

Measuring A_{PV} determines the weak form factor $F_W(Q^2)$ and from this the neutron radius R_n [21]. The neutron skin thickness $R_n - R_p$ then follows, since R_p is known. Finally, the neutron skin thickness constrains the density dependence of the symmetry energy [22, 23, 24]

Recently, the Lead Radius Experiment (PREX) at Jefferson Laboratory has pioneered parity violating measurements of neutron radii and demonstrated excellent control of systematic errors [25]. The experimental configuration for PREX is similar to that used previously for studies of the weak form factor of the proton and ^{4}He [26]. The Thomas Jefferson National Accelerator Facility provided excellent beam quality, while the large spectrometers in Hall A allowed PREX to separate elastically and inelastically scattered electrons and to greatly reduce backgrounds.

In this contribution we discuss the PREX-I result [25] and the follow-on measurement PREX-II [27] and the CREX proposal for ^{48}Ca [28]. These experiments PREX-II and CREX should measure neutron skins with high accuracy.

2   Experimental Method

The experiments run at Jefferson Lab using the high-resolution spectrometers (HRS) [29] in Hall A, comprising a pair of 3.7 msr spectrometer systems with 10^{-4} momentum resolution, which focus elastically scattered electrons onto total-absorption detectors in their focal planes.

A polarized electron beam scatters from a target foil, and ratios of detected flux to beam current integrated in the helicity period are formed (so-called "flux integration"), and the parity–violating asymmetry in these ratios computed from the helicity–correlated difference divided by the sum (eq 1). Separate studies at lower rates are required to measure backgrounds, acceptance, and Q^2. Polarization is measured once a day by a Møller polarimeter, and monitored continuously with the Compton polarimeter.

The asymmetry is small, of the order of one or two parts per million (ppm) for the kinematics of interest for the two nuclei under primary consideration namely, ^{208}Pb (PREX) and ^{48}Ca (CREX). To have significant impact on our knowledge of skin thicknesses, A_{PV} must be measured with a precision in the range of 3% or better (see fig 2). Experiments of this nature are optimized to the challenges of precision measurement of very small asymmetries, which require high count rates and low noise to achieve statistical precision as well as a careful regard for potential systematic errors associated with helicity reversal, which must be maintained below the 10^{-8} level.

One common feature of all measurements of parity-violation in electron scattering is a rapid flipping of the electron beam helicity, allowing a differential measurement

between opposing polarization states on a short timescale. The enabling technology for these measurements lies in the semiconductor photo-emission polarized electron source, which allows rapid reversal of the electron polarization while providing high luminosity, high polarization, and a high degree of uniformity between the two beam helicity states. Developments with the polarized source at Jefferson Lab are critical to the success of this program [30].

In a parity experiment, the asymmetry generally increases with Q^2 while the cross section decreases, which leads to an optimum choice of kinematics. For parity-violating neutron density experiments, the optimum kinematics is the point which effectively minimizes the error in the neutron radius R_n. This is equivalent to maximizing the following product, which is the figure-of-merit (FOM)

$$FOM = R \times A^2 \times \epsilon^2 \tag{5}$$

Here, R is the scattering rate, A is the asymmetry, $\epsilon = \frac{dA/A}{dR_n/R_n}$ is the the sensitivity of the asymmetry for a small change in R_n, dR_n/R_n is a fractional change in R_n and dA/A is a corresponding fractional change in A. Note that the FOM defined for many types of parity-violation experiments is $R \times A^2$, but the neutron-density measurements must also fold in the sensitivity ϵ.

Given practical constraints on the solid angle of the HRS, the optimization algorithm favors smaller scattering angles. Using septum magnets we reach $\sim 5°$ scattering angle. Once the angle is fixed, the optimum energy for elastic scattering can be specified. Simulations that are performed to design the experiment include the Coulomb distortions, as well as radiative losses, multiple scattering, and ionization losses in materials, together with a model for the tracking of particle trajectories through the HRS and septum magnets.

The two nuclei of interest for 1%, or better, R_n measurements (^{48}Ca and ^{208}Pb) are equally accessible experimentally and have been very well studied [1, 31, 32, 33, 34]. These are doubly-magic and have a simple nuclear structure, making them good candidates for extracting the symmetry energy. Each nucleus has the advantage that it has a large splitting to the first excited state (2.60 MeV for ^{208}Pb and 3.84 MeV for ^{48}Ca), thus lending themselves well to the use of a flux integration technique.

To achieve the 10^{-8} statistical precision and systematic control for A_{PV} measurements requires a precise control and evaluation of systematic errors, as has been developed at Jefferson Lab [26] and elsewhere [35]. PREX-I was able to achieve overall asymmetry corrections due to helicity-correlated beam position fluctuations of about 40 ppb with position differences < 5 nm. The position/asymmetry correlations are measured using two independent methods: first, directly observing the asymmetry correlations by the natural beam motion and second, by systematically perturbing the beam through a set of magnetic coils (dithering). Achieving these small values for the differences was possible in part by periodically inserting the half-wave plate
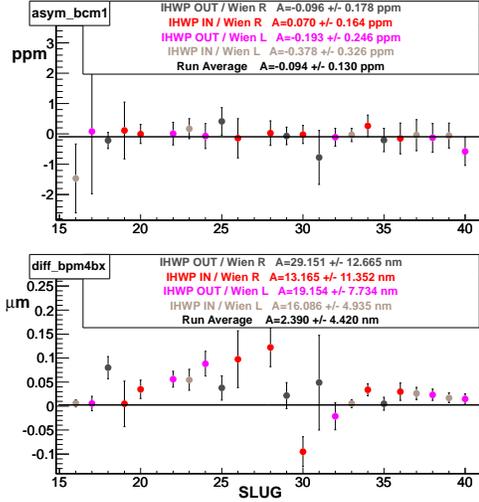
3

Figure 1: PREX-I helicity-correlated charge asymmetries (top) and position differences (bottom) on a representative monitor versus slug (a slug is ~ 1 day of running). The different colors correspond to four different combinations of insertable halfwave plate (IHWP) and Wien used for slow sign reversal, as explained in the text. To illustrate the systematics, the data points are plotted without sign correction for the helicity flip. The final average with all sign corrections is shown by the black horizontal bar and was controlled at the 5 nm level averaged over the PREX-I run. The charge asymmetry was forced to zero by the standard feedback system.

in the injector and flipping the helicity of the beam using a double-Wien filter which helps them cancel over time. Fig 1 shows the helicity-correlated charge asymmetries and position differences versus time during PREX-I. A beam current monitor (BCM) and one representative beam position monitor (BPM) is shown; the other BPMs look similar. Feedback on the charge asymmetry forced it to be zero within 0.13 ppm. The utility of the slow reversals is demonstrated in the BPM difference plot; without them, the position differences remained at the ~ 50 nm level (the points without sign correction) averaged over the experiment; with the reversals, the differences averaged to the ~ 5 nm level (the black lines) and became a negligible correction [36, 37, 38, 39, 40].

3 PREX-I Result and PREX-II Motivation

PREX-I ran in 2010 and demonstrated successful control of systematic errors, overcoming many technical challenges, but encountered significant loss of beam time due to difficulties with vacuum degradation of the target region due to the high radiation environment [25]. PREX-II is an approved experiment for a followup measurement with anticipated improvements to take data at a rate equivalent to the original
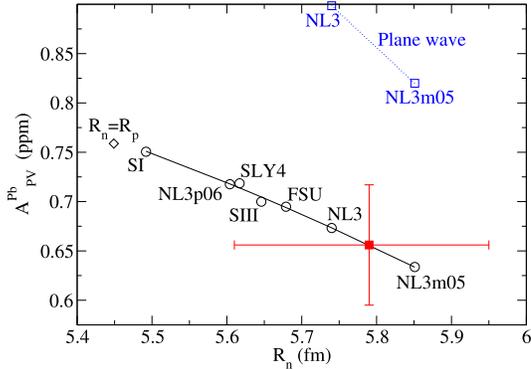
Figure 2: Result of the PREX-I experiment (red square) vs neutron point radius R_n in ^{208}Pb. Distorted-wave calculations for seven mean-field neutron densities are circles while the diamond marks the expectation for $R_n = R_p$ [41]. References: NL3m05, NL3, and NL3p06 from [42], FSU from [43], SIII from [44], SLY4 from [45], SI from [46]. The blue squares show plane wave impulse approximation results.

proposal estimates [27]. PREX measures the parity-violating asymmetry A_{PV} for 1.06 GeV electrons scattered by about five degrees from ^{208}Pb. A major achievement of PREX-I, despite downtimes mentioned above, was control of the systematic error in A_{PV} at the 2% level.

The result from PREX-I was [25]

$$A_{PV} = 0.656 \pm 0.060(\text{stat}) \pm 0.014(\text{syst}) \text{ ppm} \,. \tag{6}$$

This result is displayed in Figure 2, in which models predicting the point-neutron radius illustrate the correlation of A_{PV}^{Pb} and R_n [41]. For this figure, seven non-relativistic and relativistic mean field models [42, 43, 44, 45, 46] were chosen that have charge densities and binding energies in good agreement with experiment, and that span a large range in R_n. The weak charge density ρ_w was calculated from model point proton ρ_p and neutron ρ_n densities, $\rho_w(r) = q_p\rho_{ch}(r) + q_n \int d^3r'[G_E^p\rho_n + G_E^n\rho_p]$, using proton $q_p = 0.0721$ and neutron $q_n = -0.9878$ weak charges that include radiative corrections. Here G_E^p (G_E^n) is the Fourier transform of the proton (neutron) electric form factor. The Dirac equation was solved [19] for an electron scattering from ρ_w and the experimental ρ_{ch} [1], and the resulting $A_{PV}(\theta)$ integrated over the acceptance to yield the open circles in Fig. 2. The importance of Coulomb distortions is emphasized by indicating results from plane-wave calculations, which are not all contained within the vertical axis range of the figure.

5

Table 1: Parameters of the PREX (I and II) and CREX experiments.

	PREX	CREX
Energy	1.0 GeV	2.2 GeV
Angle	5 degrees	4 degrees
A_{PV}	0.6 ppm	2 ppm
1st Ex. State	2.60 MeV	3.84 MeV
beam current	70 μA	150 μA
rate	1 GHz	100 MHz
run time	35 days	45 days
A_{PV} precision	9% (PREX-I) 3% (PREX-II)	2.4%
Error in R_N	0.06 fm (PREX-II)	0.02 fm

4   CREX Proposal

The ^{48}Ca Radius EXperiment (CREX) was recently approved by the program advisory committee at Jefferson Lab [28]. The experiment plans to measure the parity-violating asymmetry for elastic scattering from ^{48}Ca at E = 2.2 GeV and $\theta = 4°$. This will provide a measurement of the weak charge distribution and hence the neutron density at one value of $Q^2 = 0.022$ (GeV/c)^2. It will provide an accuracy in the ^{48}Ca neutron radius R_n^{48} equivalent to ± 0.02 fm ($\sim 0.6\%$). A measurement this precise will have a significant impact on nuclear theory, providing unique experimental input to help bridge ab-initio theoretical approaches (based on nucleon-nucleon and three-nucleon forces) and the nuclear density functional theory (based on energy density functionals) [28, 48] Together with the PREX measurement of R_n^{208}, CREX (R_n^{48}) will provide unique input in such diverse areas such as neutron star structure, heavy ion collisions, and atomic parity violation. A precise measurement on a small nucleus is favorable because it can be measured at high momentum transfer where the asymmetry is larger (for the proposed kinematics, about 2 ppm). Also, since ^{48}Ca is neutron-rich it has a relatively large weak charge and greater sensitivity to R_n.

The significant new apparatus elements for CREX are the 1 gm/cm^2 ^{48}Ca target and a new 4° septum magnet. The rest of the apparatus is standard equipment and the methods of section 2 are applied. The experiment is designed for 150 μA and a 2.2 GeV beam energy, which is a natural beam energy at Jefferson Lab (1-pass through the accelerator). At this energy, the figure-of-merit, which is the total error in R_n including systematic error, optimizes at a scattering angle of 4°. Table 1 highlights the experimental configuration and goals of PREX and CREX.

5   Conclusion

In this contribution we discussed the future measurements PREX-II and CREX at Jefferson Lab. The parity-violating electron scattering asymmetry from ^{208}Pb and ^{48}Ca provide a clean measurement at one Q^2 of the weak charge of these nuclei and are sensitive to the nuclear symmetry energy. The experiments leverage the advantages Jefferson Lab, with it's highly stable and precisely controlled electron beam and the high resolution spectrometers, which are uniquely suited to perform these experiments. Within the next few years, these R_n measurements on ^{208}Pb and ^{48}Ca will provide powerful experimental inputs to tune nuclear models of increasing sophistication.

PREX-I achieved the first electroweak observation, at the 1.8σ level, of the neutron skin of ^{208}Pb and successfully demonstrated this technique for measuring neutron densities, with an excellent control of systematic errors. The future PREX-II run will reduce the uncertainty by a factor of three, to ± 0.06 fm in R_n. While PREX-II will put a constraint on the density dependence of the symmetry energy (the parameter L), models predicting neutron radii of medium mass and light nuclei are affected by nuclear dynamics beyond L. CREX will provide new and unique input into the isovector sector of nuclear theories, and the high precision measurement of R_n (± 0.02 fm) in a doubly-magic nucleus with 48 nucleons will help build a critical bridge between ab-initio approaches and nuclear DFT. CREX results can be directly compared to new coupled cluster calculations sensitive to three neutron forces [48].

References

[1] B. Frois et al., Phys. Rev. Lett. **38**, (1977) 152.

[2] H. De Vries *et al.*, Atomic and Nuc. Data Tables, **36** (1987) 495.

[3] I. Angelia and K.P. Marinova, Atomic and Nuc. Data Tables, **99** (2013) 69.

[4] C. Garcia-Recio, J. Nieves, E. Oset, Nucl. Phys. A **547**, (1992) 473.

[5] L. Ray, W. R. Coker, G.W. Hoffmann, Phys. Rev. C **18**, (1978) 2641.

[6] V.E. Starodubsky, N.M. Hintz, Phys. Rev. C **49**, (1994) 2118.

[7] B.C. Clark, L.J. Kerr, S. Hama, Phys. Rev. C **67**, (2003) 054605.

[8] A. Trzcinska *et al.*, Phys. Rev. Lett. **87**, (2001) 082501.

[9] H. Lenske, Hyperfine Interact. **194**, (2009) 277.

[10] A.M. Bernstein and W.A. Seidler, Phys. Letters **39B** no. 5 (1972) 583.

[11] A.M. Bernstein and W.A. Seidler, Phys. Letters **34B** no. 7 (1971) 569.

[12] A. Krasznahorkay *et al*, Phys. Rev. Lett. **82**, (1999) 3216; A. Krasznahorkay *at al*, Nucl. Phys. **A371**, 224 (2004).

[13] J. Piekarewicz, arXiv:1307.7746 [nucl-th].

[14] M. Warda, X. Vinas, X. Roca-Maza, M. Centelles, Phys. Rev. C **80** (2009) 024316.

[15] P. Danielewicz, Nulc. Phys. **A 727** (2003) 233.

[16] Kelly Patton, Jonathan Engel, Gail C. McLaughlin, Nicolas Schunck, ArXiv:1207.0693 (2012).

[17] C. J. Horowitz, K. J. Coakley, D. N. McKinsey, Phys. Rev. D **68** (2003) 023005.

[18] T.W. Donnelly, J. Dubach, I. Sick, Nucl. Phys.A **503**, (1989) 589.

[19] C.J. Horowitz, Phys. Rev. C **57** , (1998) 3430.

[20] C.J. Horowitz, S.J. Pollock, P.A. Souder, R. Michaels, Phys. Rev. C **63**, (2001) 025501.

[21] C.J. Horowitz, *et al.*, Phys. Rev. C **85**, (2012) 032501.

[22] X. Roca-Maza, *et al.*, arXiv:1307.3879 [nucl-th]; *ibid*, Phys. Rev. Lett **106**, (2011) 252501.

[23] X. Vinas, M. Centelles, X. Roca-Maza, and Warda arXiv:1308.1008 [nucl-th].

[24] "Topical Issue on Nuclear Symmetry Energy", EPJA **50** 2 (2014).

[25] S. Abrahamyan *et al.*, Phys. Rev. Lett. 108, (2012) 112502.

[26] K. A. Aniol *et al.*, Phys. Rev. Lett. **82** 1096 (1999) 1096; K. A. Aniol, *et al.*, Phys. Rev. C 69, (2004) 065501; K. A. Aniol, *et al.*, Phys. Rev. Lett. **96** (2006) 022003; K. A. Aniol, *et al.*, Phys. Rev. Lett. **98** (2007) 032301; Z. Ahmed, *et al.*, Phys. Rev. Lett. **108** (2012) 102001.

[27] The PREX-II proposal, unpublished, available at hallaweb.jlab.org/parity/prex.

[28] The CREX proposal, unpublished, available at hallaweb.jlab.org/parity/prex.

[29] J. Alcorn *et al.*, Nucl. Instrum. Meth. A **522**, (2004) 294.

[30] C. K. Sinclair, *et al.* Phys. Rev. ST Accel. Beams 10, (2007) 023501; P.A. Adderley, *et al.* Phys. Rev. ST Accel. Beams 13, (2010) 010101.

[31] J.E. Wise *et al.*, Phys. Rev. C 31, (1985) 1699.

[32] J.M. Cavedon, *et al.* Phys. Rev. Lett **58** 1987 195.

[33] H.J. Emrich, *et al.* Nucl. Phys. A **396** (1983) 401C.

[34] E.N.M Quint, *et al.* Phys. Rev. Lett **57** (1986) 186.

[35] T. B. Humensky, R. Alley, A. Brachmann, M. J. Browne, J. Clendenin, J. de-Lamare, J. Frisch and T. Galetto *et al.*, Nucl. Instrum. Meth. A **521** (2004) 261.

[36] Kiadtisak Saenboonruang, PhD Thesis, University of Virginia (2012) unpublished.

[37] Rupesh Silwal, PhD Thesis, University of Virginia (2012) unpublished.

[38] Luis R. Mercado, PhD Thesis, University of Massachusetts (2012) unpublished.

[39] Chun-Min Jen, PhD Thesis, Syracuse University (2012) unpublished.

[40] Zafar Ahmed, PhD Thesis, Syracuse University (2012) unpublished.

[41] S. Ban, C.J. Horowitz, R. Michaels, J. Phys G **39**, (2012) 015104.

[42] G. A. Lalazissis, J. Konig, and P. Ring, Phys. Rev. C**55**, (1997) 540.

[43] B.G. Todd-Rutel, J. Piekarewicz, Phys. Rev. Lett. **95**, (2005) 122501.

[44] M. Beiner, H. Flocard, N. Van Giai, P. Quentin, Nucl. Phys. A **238**, (1975) 29.

[45] E. Chabanat, P. Bonche, P. Haensel, J. Meyer, R. Scha- er, Nucl. Phys. A **635**, (1998) 231.

[46] D. Vautherin, D. M. Brink, Phys. Rev. C **5**, (1972) 626.

[47] http://www.jlab.org/conferences/crex/

[48] G. Hagen *et al.*, arXiv::1509.07169 (2015).